Online Journal of Space Communication

Satellite Imagery in the Study and Forecast of Malaria

David J. Rogers

Sarah E. Randolph

Robert W. Snow

Simon I. Hay

Follow this and additional works at: https://ohioopen.library.ohio.edu/spacejournal

🟡 Part of the Astrodynamics Commons, Navigation, Guidance, Control and Dynamics Commons, Space Vehicles Commons, Systems and Communications Commons, and the Systems Engineering and Multidisciplinary Design Optimization Commons

Recommended Citation

Satellite Imagery in the Study and Forecast of Malaria

David J. Rogers, Sarah E. Randolph, Robert W. Snow, and Simon I. Hay

The authors are affiliated with the following: TALA Research Group and Oxford Tick Research Group, Department of Zoology, University of Oxford; Kenya Medical Research Institute/Wellcome Trust Collaborative Programme, Nairobi, Kenya; and the Centre for Tropical Medicine, University of Oxford, John Radcliffe Hospital.

More than 30 years ago, human beings looked back from the Moon to see the magnificent spectacle of Earthrise. The technology that put us into space has since been used to assess the damage we are doing to our natural environment and is now being harnessed to monitor and predict diseases through space and time. Satellite sensor data promise the development of early-warning systems for diseases such as malaria, which kills between 1 and 2 million people each year.

1. Introduction

Malaria caused by Plasmodium falciparum parasites exacts its greatest toll in sub-Saharan Africa, where it is one of the largest causes of morbidity and mortality, creating a significant barrier to economic development. Furthermore, this public health burden is increasing globally,[1] exacerbated by failure of existing affordable drugs, population growth against declining per capita expenditure on health, human migration and poverty. As a step towards reversing this trend, there is growing interest in the mapping and predictive modelling of the geographical limits, intensity and dynamics of the risk of malaria infection, using new tools of surveillance. An unprecedented amount of information on environmental conditions, remotely sensed by satellite sensors, is now available at temporal and spatial resolutions to match our epidemiological questions.

Here we show how these tools are used to investigate the factors that drive the dynamics of vector populations and malaria parasite transmission. Because mosquito population processes and malaria incubation periods in vectors, for example, vary with temperature and moisture conditions on the ground, remotely sensed images of seasonal climate are powerful predictors of mosquito distribution patterns and average levels of transmission of malaria parasites by these vectors. Patterns of infection vary through time owing to extrinsic (for example, climate) and intrinsic (for example, immunity) effects. The balance of these factors depends upon the levels of malaria transmission in each place and will change over time with resistance to control of parasites and vectors. Early-warning systems, therefore, will require models that incorporate both intrinsic and extrinsic factors.

2. Extrinsic and Intrinsic Drivers of Malaria

Diseases caused by vector-borne pathogens vary in magnitude through space and time much more than directly transmitted pathogens, because their innate capacity to increase is usually much higher. This is expressed as the basic reproductive number R_0:

$$R_0 = ma^2bce^{-mT}/\mu r$$

where m is the vector-host ratio; a is the vector biting rate; b,c are transmission coefficients from vertebrate to vector and vice versa; μ is the vector mortality rate; T is the extrinsic incubation period of the parasite in the vector; and r is the rate of recovery in the vertebrate. Values of R_0 for vector-borne pathogens reach hundreds, or even thousands, compared with a typical value of <10 for directly transmitted pathogens.[2] Changes in R_0 are most sensitive to changes in variables that appear as powers or exponents (a, μ and T).[3][4]

R_0 is reduced to R_E, the effective reproductive number that approximates to 1.0 at equilibrium, by population acquired immunity and other processes that either limit vertebrate infectivity for mosquitoes or decrease coefficients of transmission between vertebrates and vectors. Thus, although the increase of vector-borne pathogens is most strongly influenced by the six (out of seven) vectorrelated factors in the R_0 equation, their regulation is effected principally by vertebrate factors. However, because acquired vertebrate immunity depends upon the level and frequency of exposure to parasites since birth, it should be possible to define the dynamics of many vector-borne pathogens solely on the basis of the current and previous history of the vector population.

Although invertebrate vectors are strongly influenced by variable climate (that is, abiotic or extrinsic factors),[5] vertebrate host immunity effects (biotic or intrinsic factors) can produce characteristic cycles of infection even in the absence of variation in environmental conditions.[6] The interaction of extrinsic and intrinsic factors results in the characteristic waxing and waning of many vector-borne infections, on timescales from weeks to decades;[7][8] these cycles may be suppressed, but are rarely totally eliminated, by control and intervention efforts. Early attempts to predict malaria outbreaks in India and Pakistan revealed an understanding of this interaction:[9] a combination of the absence of malaria in the preceding 5 years, rainfall anomalies from July to August, and the local prices of wheat (thought to reflect the nutritional state of the human population) was used to predict the amount and distribution of malaria in 1921 with 'considerable precision.'[10] This early promise of accurate forecasting of malaria outbreaks was implemented successfully in the subcontinent for almost 25 years[11] until

the introduction of insecticides and cheap drugs in the 1950s and 1960s, when forecasting was no longer felt necessary.[12] There have been no effective early-warning systems for malaria, or indeed for any vectorborne diseases, since that time.[13]

3. New Prospects for Malaria Early-Warning Systems

With a breakdown in effectiveness of the 'cures' found for malaria in the 1950s and 1960s, there has been a global resurgence of malaria1,[14][15] and renewed interest in the concept of malaria early warning.[13][16][17] But instead of rain gauges and wheat prices, we now have an armoury of information on environmental conditions, remotely sensed from satellite sensors, that has been related to the dynamics of vector populations and pathogen transmission.[18][19] Until we can dissect quantitatively the roles played by extrinsic and intrinsic factors, however, we cannot use these new tools to forecast outbreaks. First, therefore, we focus on what satellite imagery can tell us about the environmental prerequisites for malaria transmission in the equilibrium situation.

3.1 The Risk-Challenge Relationship for Malaria

The hypothetical relationship between the challenge presented to the human population by a vector population and the resulting incidence or prevalence of infection, each assuming stable conditions, is complex and nonlinear (Fig. 1). The humped curve is determined by interactions between transmission rates, the rate of development and duration of temporary acquired immunity in the vertebrate host population, and the age structure of the latter. But the precise shape of the relation, and its implications for malaria control, are controversial,[20][21] not least because of a shortage of good quality field data available for its determination. (The relationship between clinical disease and challenge may be different from that shown in Fig. 1, most obviously in areas of high challenge.) The data that do exist for Africa, now being gathered together in the ambitious Mapping Malaria Risk in Africa/Atlas du Risque de Malaria en Afrique collaboration,[22][23] may nevertheless be used first to examine the 'challenge' axis of Fig. 1.
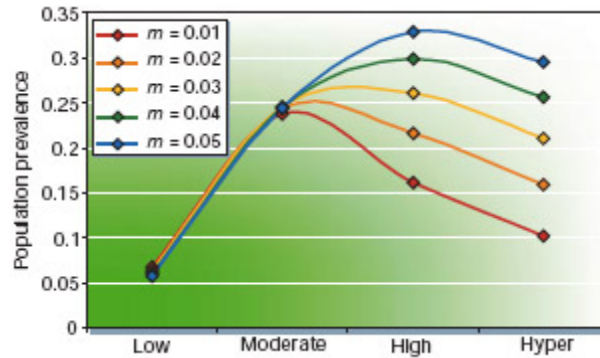
Figure 1: Hypothetical relationship between the challenge to a host population by a vector-borne pathogen and the risk of the host becoming infected. Challenge is a function of many elements of the vector's biology; risk is often modulated by host resistance and/or acquired immunity. Fixed age-specific prevalences at each level of challenge with different levels of vertebrate host mortality rate (m in the figure) produce population prevalence/challenge curves of different overall shapes.

3.2 Distribution and Abundance of Mosquito Vectors

The distribution of efficiently transmitted pathogens such as those that cause malaria is generally limited by the distribution of competent vectors, which can now be predicted from satellite imagery. In Africa, the main vectors of malaria include species of the *Anopheles gambiae* complex (*A. arabiensis, A. bwambae, A. gambiae* s.s., *A. melas, A. merus* and *A. quadriannulatus*) and *A. funestus*, whose distributions show similarities with patterns of annual rainfall across Africa.[24] Furthermore, a relationship found in West Africa between climate (annual precipitation and annual and wet-season temperatures) and the ratio of *A. gambiae* s.s. to *A. arabiensis* was used successfully to predict the distribution and relative abundance of these two species in Tanzania (East Africa).[25] The subtlety and extensive coverage of multivariate climatic factors detectable by satellite sensors have allowed predictions of the distribution of five of the six species in this complex (Fig. 2; *A. bwambae*, restricted to a small site in Uganda, is not modelled). This has been achieved using maximum likelihood methods based on the relatively few studies that identified these species separately. Thus, satellites can distinguish between the habitats of species that were, until 1956, regarded as a single species.

Satellite data show strong relationships with the density of other vectors in Africa,[2][26] but mosquito abundance has only rarely been recorded, despite its importance in R0 calculations. Until such data are collected, as a matter of urgency, we speculate that abundance will be greatest in sites with conditions near to the climatic centroids defined by the satellite data, although spatially variable, densitydependent factors may confound this prediction.

Figure 2: Distributions of five mosquito species in the Anopheles gambiae complex in Africa, predicted from temporal Fourier-processed satellite data (Box 1 on page 4) and elevation (global coverage

provided by the digital elevation model GTOPO30;
http://eros.usgs.gov/products/elevation/gtopo30.php) at a spatial resolution of 0.05°. The colour-coded probabilities42 of presence effectively indicate the environmental suitability for each species throughout the continent. Symbols indicate sample sites for each species. Between 18° N to 30° S, each species was classed as present only within 0.15° of the sites from which it has been recorded[24] and absent only from similarly sized sites where any of the other species have been recorded. Within these sites, presence pixels (300 for *A. gambiae* s.s. and *A. arabiensis* and 100 for the other species) and absence pixels (400 for all species) were chosen at random; additional randomly selected absence pixels were chosen north of 18° N (n=200) and south of 30° S (n=50). Satellite data: middle infrared, land surface temperature and normalized difference vegetation index for 1982-1998 were derived from the National Oceanographic and Atmospheric Administration's Advanced Very High Resolution Radiometer, and cold cloud duration for 1988-1999 from Meteosat High Resolution Radiometer. Satellite and elevation data for all sample pixels were subjected to k-means clustering within the Statistics Package for the Social Sciences (SPSS, Chicago) to identify up to six natural clusters each of presence and absence pixels for each mosquito species. Within maximum likelihood discriminant analysis, stepwise selection of up to ten variables was applied to maximize predictive accuracy according to the kappa statistic,[28] sensitivity and specificity (Box 1 on page 4) and to calculate the posterior probabilities[42] with which each pixel belongs to the presence or absence classes within the training set. Sites too different from any of the training set sites are assigned to a 'no prediction' class.
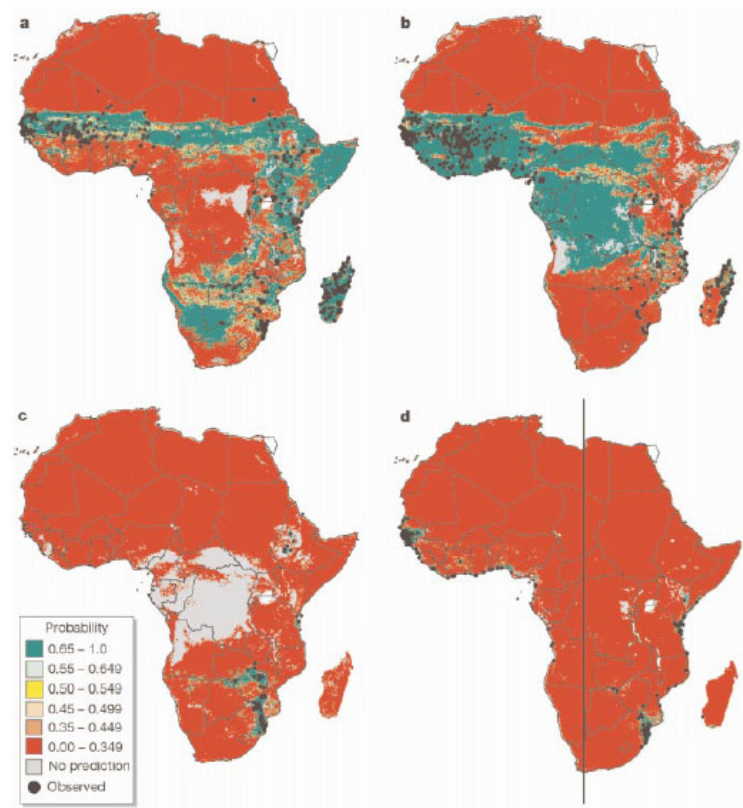
a, *A. arabiensis*: 86.0% correct predictions, 7.7% false positives, 6.2% false negatives, sensitivity=40.80, specificity=40.89, κ=40.679 (±50.051 95% confidence interval).

b, *A. gambiae* s.s.: 92.4% correct, 4.2% false positives, 3.4% false negatives, sensitivity=40.89, specificity=40.94, κ=40.826 (±50.039).

c, *A. quadriannulatus*: 99.1% correct, 0.9% false positives, 0% false negatives, sensitivity=41, specificity=40.99, κ=40.961 (±50.029).

d, *A. melas* (West Africa): 98.2% correct, 1.6% false positives, 0.1% false negatives, sensitivity=40.99, specificity=40.98, κ=40.928 ($\pm$50.039); and *A. merus* (East Africa): 98.4% correct, 1.6% false positives, 0% false negatives, sensitivity=41, specificity=40.98, κ=40.933 ($\pm$50.037).

3.3 Entomological Inoculation Rate

A more complete measure of malaria challenge is an estimate of the entomological inoculation rate (EIR), which is the product of the number of mosquito bites per human per unit time (*ma* in the R_0 equation) and the proportion of mosquitoes with sporozoites (infective stages of the malaria parasites).[3] EIRs are generally derived from short- to medium-term studies, each in a relatively small area, and are therefore of limited predictive value on their own.[27] By compiling all reliable published EIRs and relating them to satellite data, we can make more extensive predictions of this measure of challenge (Fig. 3). Analysis shows that gradual changes in environmental conditions distinguish low- and high-risk areas, and do so consistently enough for an excellent overall agreement with the field data (kappa statistic (ref. 28; and see Box 1 on page 4) of 0.77). There is also good agreement between the EIR predictions (Fig. 3) and the predicted distributions of the two key malaria vectors, *A. arabiensis* and *A. gambiae* s.s. (Fig. 2), although in parts of southern Africa, where historically vector control and case-management have been effective, present-day malaria challenge is less than is shown on this map. But many areas of Africa are too different from any of the training sets to allow any predictions for them (shown in grey in Fig. 3). By identifying these regions, satellite imagery can direct new studies of this important malariometric index.

Figure 3: Satellite-derived predictions of entomological inoculation rate (EIR) in Africa. EIR data27 (map inset) were grouped into five approximately equal-sized classes of mean levels of malaria challenge. The same satellite data layers and analytical methods as used in Fig. 2 are used to define the probability with which each continental pixel belongs to one of the five challenge categories. Insufficient training data were available to define EIR in those parts of the continent marked grey.
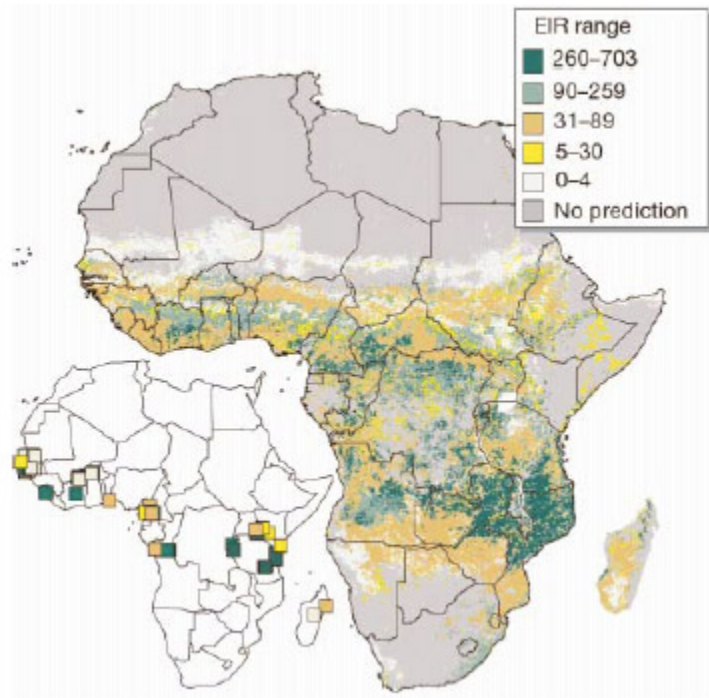
Descriptive accuracies: EIR range 0-4.4, 85.7% (n=21); 5.8-26.6, 81.8% (n=22); 31.0-87.0, 77.3% (n=22); 89.8-255.5, 68.2% (n=22), 259.9-703.4, 95.5% (n=22). Overall κ=40.771 ($\pm$50.064).

3.4 Resulting Malaria Incidence and Prevalence

Biologically, and for the purposes of intervention, the point of interest is to explain the relationship between the above three measures of challenge (mosquito distribution and abundance, and EIR) and the resulting disease burdens, and so be able to predict the latter. We are hindered from making even statistical predictions by the lack of good quality training sets for satellite studies, as disease risks have been determined too infrequently, and over insufficiently wide areas. With the aid of satellites, however, a small training set can produce predictions across a large area.

Numbers of monthly childhood malaria admissions in three hospitals in Kenya, expressed as a percentage of the annual totals, were found to be correlated most consistently (mean adjusted r^2=40.71) with the previous month's normalized difference vegetation index (NDVI), ([Box 1](#) on page 4)[29], which is related to plant photosynthetic activity. As minimum NDVIs of 0.35-0.40 were shown to be required before >5% of annual admissions were recorded in any one month, the duration of malaria transmission seasons across Kenya and Uganda could be predicted by counting the number of months in which these NDVI values were exceeded.[18][30] The resulting predictive maps of malaria seasons showed strong similarities to an historical map of malaria transmission periods in Kenya.[31]

4. Non-Equilibrium Situations

4.1 Seasonality and Intrinsic Dynamics

The position of any site on the horizontal axis of Fig. 1 determines average malaria risk, but seasonal changes in the challenge variables (mosquito abundance and EIR) cause seasonal changes in risk that may be either very pronounced (such as is characteristic of conditions of low average challenge) or strongly buffered by herd immunity responses (at high challenges). At low challenge levels, and because of time delays between the index of challenge and its expression as malaria infections, the risk-challenge relationship will trace an anticlockwise ellipse over time, completing approximately one cycle per year. Remotely sensed data that monitor one or more measure of challenge will therefore be able to predict risk with an appropriate lead time.

In high challenge areas this simple picture is obscured by the longer-term effects of intrinsic disease dynamics, which tend to be uncoupled from the annual seasonality in a way that makes prediction much less accurate. Intrinsic dynamics can produce cycles of disease prevalence in human populations with periods of a few to many years. A recent analysis of long-term records of two mosquitoborne diseases, dengue in Thailand and malaria in Kenya, shows clear evidence of such cycles, with periods in each case of about 3 years.[32] The absence of any sign of equivalent multi-annual cycles in the contemporary meteorological records at each site supports the interpretation that these cycles are driven by intrinsic biotic factors such as host acquired immunity.

The transition from low levels of endemicity, where variation in malaria incidence is apparently driven by extrinsic factors, to higher levels of endemicity, where intrinsic dynamics overrides annual seasonality, may be abrupt (D.J.R., unpublished data). This transition may occur with only modest increases in average mosquito abundance. Above a certain level of endemicity the resulting multi-annual cycles of infection are neither simply, nor easily, linked to either meteorological or satellite data.

4.2 Short- and Long-Term Cycles in Weather Patterns

Longer-term weather cycles such as the El Niño/Southern Oscillation (ENSO) in the Pacific Ocean have been invoked recently to 'explain' outbreaks of malaria and other diseases.[33] Some of these analyses are not statistically robust, while none of them allows an alternative explanation involving intrinsic cycles. This problem is particularly acute because within the past 30-40 years the quasiperiodic ENSO signal has shown a gradual increase in frequency and now has a periodicity of approximately four years.[34] This is close enough to the intrinsic cycles revealed for dengue in Thailand and malaria in Kenya for a casual analysis to suggest a causal link between the two. Before any disease periodicity can be attributed with any certainty to ENSO, a link must be established between

the global ENSO index and local weather records (measured directly or remotely) pertinent to the particular vector-borne pathogen.

4.3 Trends and Global Change

The disparity in conclusions about the likely impact of global climate change on malaria distribution in the future [35][36] highlights the significant gaps in our knowledge of this most important tropical disease. Attempts to relate past trends in malaria prevalence to climate records[37] are the critical tests of the real role of climate in the recent history of malaria and therefore its likely impact in the future. Statistical analyses of time series usually require stationarity (the property of constant mean and variance through a series), which is generally achieved by calculating the difference from the overall trend line of each sequential observation. Often, however, it is the trend itself which is of interest and importance.

Windowed Fourier analysis (Box 1 on page 4) of long-term (1966-1998) monthly malaria data from Kericho, Kenya[32][38] shows that the amplitude of many of the component Fourier harmonics has increased over this period; this is most marked in cycles with periods of one and about three years (Fig. 4). Similar analyses of contemporary temperature and rainfall records show no equivalent changes (Fig. 4); rather, if anything there has been a decrease in the amplitude of the same Fourier harmonics. The most parsimonious interpretation of these results is that following a period of aggressive and wide-spread use of chloroquine for fever management, and for some periods as prophylaxis, this drug became less effective at parasite clearance during the mid-late 1980s. Malaria no longer suppressed by the drugs began to show higher-amplitude extrinsic and intrinsic cycles, coupled, respectively, to annual seasonal variation and infection-recovery-immunity effects.

Where climate change is accompanied by changing abundance of mosquitoes, its impact on the levels and periodicity of malaria outbreaks will be far more complex than modelled so far. Although remotely sensed images of seasonal environments can set the scene for long-term studies of disease, such data must be combined with contemporary field data and dynamic models of disease transmission for a full explanation of vector-borne diseases in an ever-changing world.

Figure 4: Amplitude of Fourier harmonics derived from windowed Fourier analysis of malaria cases per month and a range of climatic variables for the period January 1966 to December 1998.
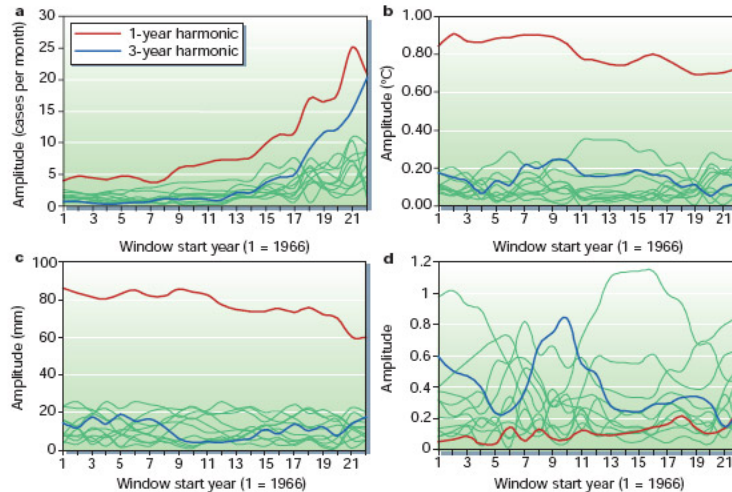
a, Malaria cases per month;

b, temperature (°C);

c, rainfall (mm); data (from ref. 38) from Kericho, Kenya.

d, Data from the Multivariate El Niño/ Southern Oscillation (ENSO) Index[43][44] (
http://www.cdc.noaa.gov/people/klaus.wolter/MEI/).

All data were first de-trended with a 60-point moving average, and the analysis was based upon the difference of the raw data from this trend line. Beginning in 1966, a 12-year window was moved forward one year at a time until 1998 was included. The rapid increase in the amplitudes of the 1-year (red line) and ~3-year (blue line) harmonics of the malaria data have no obvious parallels in the temperature, rainfall or ENSO records, suggesting that these changes are not driven by any element of climate change. The green lines show the results for all other harmonics with periods of between 1 and 12 years.

<hr>

5. Future Perspectives

Statistical models relating various components of the transmission of malaria parasites to satellite data demonstrate clearly the potential role and importance of remotely sensed imagery to descriptions, explanations and predictions of vector-borne disease. In the face of a world changing in both abiotic and biotic respects, and complex infection and disease dynamics that are not amenable to simple statistical interpretations, we must now take the next step -- the incorporation of satellite data into biological models of pathogen transmission. Studies have already related vector mortality rates and abundance to satellite data,[39] and biological models have been developed for a few vectors[40][41] and vector-borne pathogens.[26]

Extensive satellite coverage coupled with vector-borne pathogen models that are appropriate at a local scale will enable us to build spatially rich, accurate models of vector-borne pathogens. If we can understand transmission dynamics well enough to model the present, we should be able to develop accurate disease early-warning systems in the future. It is clear that the technologies we now have to study these diseases are far better than those available to malariologists in the

early years of the last century. The challenge is to make the science of malaria prediction at least as good.

Box 1: Satellite Sensors for Monitoring Diseases

Satellite sensor designs are rarely ideal for epidemiological studies because of trade-offs between spectral, spatial and temporal resolution, determined by constraints of the Earth's atmosphere, or the original requirements of commissioning agencies. Passive satellite sensor data (that is, reflections or emissions arising ultimately from the Sun) have been used most commonly for epidemiological studies, and are discussed here, but there is increasing interest in radar satellites with active sensors that can produce images even under cloudy conditions.

Spectral Resolution

Satellite sensors detect reflected sunlight or infrared radiation emitted by all bodies above absolute zero. Data are most readily available in three to seven wavebands or channels in the humanvisible and near-to-thermal infrared part of the electromagnetic spectrum (0.3-14-µm wavelengths).

Spatial Resolution

Earth-observing satellites produce data with spatial resolutions of 1-4 m (Ikonos-2), 10-20 m (Satellite pour l'Observation de la Terre; SPOT), 30-120 m (Landsats 1-5) or 15-60 m (Landsat 7). Images, made up of picture elements or 'pixels' of these sizes, have swath widths of ˜11 km (Ikonos), ˜60 km (SPOT) and 185 km (Landsat). The 'vegetation instrument' on SPOT-4 has a spatial resolution of 1 km and a 2,250-km swath width.

Meteorological satellites have lower spatial resolutions, with pixel sizes down to 1.1 km (National Oceanographic and Atmospheric Administration Advanced Very High Resolution Radiometer; NOAAAVHRR), and a correspondingly wider swath width of ˜2,400 km. Geostationary satellites maintain a constant position relative to the Earth, giving spatial resolutions of 1-8 km (Geostationary Operational Environmental Satellite for the Americas) or 2.5-5 km (Meteosat 4-6 for Europe/Africa) and images of the entire Earth halfdisk.

Temporal Resolution

Satellites with a higher spatial resolution have a repeat frequency of 11 (Ikonos), 16 (Landsat) or 26 (SPOT) days. Orbiting meteorological satellites produce two images per day of the entire Earth's surface, whereas geostationary satellites produce two images per hour to monitor weather systems.

New Satellites and Sensors

New systems promise greater spectral and spatial resolutions, and greater signal stability over time. These include the Moderate Resolution Imaging Spectrometer on the Terra spacecraft (http://terra.nasa.gov), and the Spinning Enhanced Visible and Infrared Imager on the geostationary Meteosat Second Generation (http://www.esa.int).

Images for Epidemiology

Imagery is adversely affected by atmospheric contamination such as clouds and other aerosols. The low repeat frequency of the higher spatial resolution satellites prevents the recording of important seasonal determinants of pathogen transmission rates. In contrast, frequent images from NOAA-AVHRR and Meteosat sensors can be combined to produce relatively cloud-free monthly images generated from the maximum values of each signal recorded during the period (assumed to reflect cloud-free conditions), called maximum value composites.[18] These are of much greater use in studying dynamical epidemiological processes.

Data from each satellite channel may be used directly to describe epidemiological events, or may be processed to produce indices related to ground-based variables such as soil surface temperatures. Commonly used products include the middle infrared band, derived from AVHRR channel 3, and land surface temperature (LST), derived from AVHRR channels 4 and 5, both of which are related to the Earth's surface temperature; the normalized difference vegetation index, derived from AVHRR channels 1 and 2 and related to plant photosynthetic activity; near-surface air temperature, derived from LST and vegetation index measurements; and cold cloud duration from Meteosat, which is correlated with rainfall in convective precipitation systems (all reviewed in refs 18, 45).

Data Processing and Application

Monthly composited imagery often shows strong serial correlations, and therefore data redundancy, which may be overcome in two ways. The data may be subjected either to principal components analysis (PCA) and the resultant significant principal components used in further analyses, or to temporal Fourier analysis that describes natural cycles in terms of annual, bi-annual, tri-annual, and so on, components with longer or shorter periods. Temporal Fourier processing removes data redundancy and produces a set of orthogonal (uncorrelated) outputs while retaining a description of seasonality (which is lost in PCA); this is of vital interest in epidemiology.[26][46][47] Windowed Fourier analysis overcomes the problem of serial changes in the mean and variance of the data. Trends are first removed by taking the difference of the time series from a moving average spanning a number of annual cycles, and this de-trended time series is then Fourier-analysed. To deal with changing variances, a fixed aperture window is moved progressively over the de-trended time series, and only the data within the window are analysed. By comparing such analyses across the entire time series,

the periodicities contributing most to changes in the overall variance can be identified (Fig. 4 on page 3).

Composited, multi-temporal and Fourier-processed satellite sensor data may be used to describe epidemiological data statistically using linear and logistic regression techniques[48][49] or various discriminant analysis and maximum likelihood approaches.[26][50] Output maps record the similarity of each pixel to the satellite-determined environmental characteristics in a sample set of sites where the epidemiological situation is well documented (the training set). Such maps can record the predicted suitability of each pixel for the presence of a vector or disease (Fig. 2 on page 2), or quantitative data related to the burden of disease (Fig. 3 on page 2).

Predictive accuracy can be assessed using a contingency table that compares the training set data and the suitability category to which the pixels were assigned. From this is calculated the overall percentage of correct predictions, the percentage of false positives and false negatives (that is, false predictions of presence and absence, respectively), and the sensitivity and specificity (proportion of positives or negatives, respectively, correctly identified). The kappa index of agreement, k, measures predictive accuracy compared with a null model (that is, one with no predictive skill); values vary between 0 (fit no better than random) and 1.0 (perfect fit),[28] with a valuse of more than 0.75 regarded as excellent; confidence intervals can be attached to k values. Once robust and reliable correlations between the satellite and disease data are established, real-time monitoring of environmental conditions by satellites can provide valuable inputs into disease early-warning systems.[16]

Contact

David J. Rogers
TALA Research Group
Department of Zoology
University of Oxford
South Parks Road
Oxford OX1 3PS, UK
Email: david.rogers@zoo.ox.ac.uk

REFERENCES

1. Snow, R. W., Trape, J.-F. & Marsh, K. Childhood malaria mortality in Africa: past, present and future.

   Trends Parasitol. 17, 593-597 (2001).

2. Rogers, D. J. Satellite imagery, tsetse and trypanosomiasis in Africa. Prev. Vet. Med. 11, 201-220 (1991).
3. Macdonald, G. The Epidemiology and Control of Malaria (Oxford Univ. Press, London, 1957).
4. Onori, E. & Grab, B. Indicators for the forecasting of malaria epidemics. Bull. World Health Organ. 58, 91-98 (1980).
5. Hay, S. I., Tucker, C. J., Rogers, D. J. & Packer, M. J. Remotely sensed surrogates of meteorological data for the study of the distribution and abundance of arthropod vectors of disease. Ann. Trop. Med. Parasitol. 90, 1-19 (1996).
6. Anderson, R. M. & May, R. M. Infectious Diseases of Humans: Dynamics and Control (Oxford Univ. Press, Oxford, 1991).
7. Yacob, K. B. M. & Swaroop, S. Investigation of long-term periodicity in the incidence of epidemic malaria in the Punjab. J. Malaria Instit. India 6, 39-51 (1945).
8. Rogers, D. J. The dynamics of vector-transmitted diseases in human communities. Phil. Trans. R. Soc. Lond. B 321, 513-539 (1988).
9. Christophers, S. R. Epidemic malaria of the Punjab, with a note on a method of predicting epidemic years. Paludism 2, 17-26 (1911).
10. Gill, C. A. The prediction of malaria epidemics. Ind. J. Med. Res. 10, 1136-1143 (1923).
11. Swaroop, S. Forecasting of epidemic malaria in the Punjab, India. Am. J. Trop. Med. 29, 1-17 (1949).
12. Najera, J. A., Kouznetsov, R. L. & Delacollette, C. Malaria Epidemics: Detection and Control Forecasting and Prevention (World Health Organization, Geneva, 1998).
13. National Research Council. Under the Weather: Climate, Ecosystems, and Infectious Disease (Committee on Climate, Ecosystems, Infectious Diseases, and Human Health, Board on Atmospheric Sciences and Climate, National Research Council, Washington DC, 2001).
14. Snow, R. W., Craig, M., Deichmann, U. & Marsh, K. Estimating mortality, morbidity and disability due to malaria among Africa's non-pregnant population. Bull. World Health Organ. 77, 624-640 (1999).
15. World Health Organization. The World Health Report 1999: Making a Difference (World Health Organization, Geneva, 1999).
16. Myers, M. F., Rogers, D. J., Cox, J., Flauhalt, A. & Hay, S. I. Forecasting disease risk for increased epidemic preparedness in public health. Adv. Parasitol. 47, 309-330 (2000).
17. World Health Organization. Malaria Early Warning Systems, a Framework for Field Research in Africa: Concepts, Indicators and Partners (World Health Organization, Geneva, 2001).
18. Hay, S. I. An overview of remote sensing and geodesy for epidemiology and public health application. Adv. Parasitol. 47, 1-35 (2000).
19. Hay, S. I., Omumbo, J., Craig, M. & Snow, R. W. Earth observation, geographic information systems and Plasmodium falciparum malaria in sub-Saharan Africa. Adv. Parasitol. 47, 173-215 (2000).
20. Snow, R. W. & Marsh, K. Will reducing Plasmodium falciparum transmission alter malaria mortality among African children? Parasitol. Today 11, 188-190 (1995).
21. Smith, T. A., Leuenberger, R. & Lengeler, C. Child mortality and malaria transmission intensity in Africa. Trends Parasitol. 17, 145-149 (2001).
22. Mapping Malaria Risk in Africa/Atlas du Risque de Malaria en Afrique (MARA/ARMA) collaboration. Towards an Atlas of Malaria Risk in Africa. First Technical Report of the MARA/ARMA (Mapping Malaria Risk in Africa) Collaboration (MARA/ARMA, Durban, 1998).
23. Craig, M. H., Snow, R. W. & le Sueur, D. A climate-based distribution model of malaria transmission in sub-Saharan Africa. Parasitol. Today 15, 105-111 (1999).

24. Coetzee, M., Craig, M. H. & le Sueur, D. Distribution of African malaria mosquitoes belonging to the Anopheles gambiae complex. Parasitol. Today 16, 74-77 (2000).

25. Lindsay, S. W., Parson, L. & Thomas, C. J. Mapping the ranges and relative abundance of the two principal African malaria vectors, Anopheles gambiae sensu stricto and An. arabiensis, using climate data. Proc. R. Soc. Lond. B 265, 847-854 (1998).

26. Rogers, D. J. Satellites, space, time and the African trypanosomiases. Adv. Parasitol. 47, 129-171 (2000).

27. Hay, S. I., Rogers, D. J., Toomer, J. F. & Snow, R. W. Annual Plasmodium falciparum entomological inoculation rates (EIR) across Africa: literature survey, internet access and review. Trans. R. Soc. Trop. Med. Hyg. 94, 113-127 (2000).

28. Congalton, R. G. A review of assessing the accuracy of classifications of remotely sensed data. Rem. Sens. Environ. 37, 35-46 (1991).

29. Hay, S. I., Snow, R. W. & Rogers, D. J. Predicting malaria seasons in Kenya using multitemporal meteorological satellite sensor data. Trans. R. Soc. Trop. Med. Hyg. 92, 12-20 (1998).

30. Hay, S. I., Snow, R. W. & Rogers, D. J. From predicting mosquito habitat to malaria seasons using remotely sensed data: practice, problems and perspectives. Parasitol. Today 14, 306-313 (1998).

31. Butler, R. J. Atlas of Kenya: A Comprehensive Series of New and Authenticated Maps Prepared from the National Survey and other Governmental Sources with Gazetteer and Notes on Pronunciation and Spelling (The Survey of Kenya, Nairobi, 1959).

32. Hay, S. I. et al. Etiology of interepidemic periods of mosquito-borne disease. Proc. Natl Acad. Sci. USA 97, 9335-9339 (2000).

33. Kovats, R. S., Bouma, M. J. & Haines, A. El Niño and Health (World Health Organization, Geneva, 1999).

34. McGregor, G. R. & Nieuwolt, S. Tropical Climatology (Wiley, Chichester, 1998).

35. Martens, W. J. M. et al. Climate change and future populations at risk of malaria. Global Environ. Change 9, S89-S107 (1999).

36. Rogers, D. J. & Randolph, S. E. The global spread of malaria in a future, warmer world. Science 289, 1763-1766 (2000).

37. Hay, S. I. et al. Climate change and the resurgence of malaria in the East African highlands. Nature (in the press).

38. Shanks, G. D., Biomndo, K., Hay, S. I. & Snow, R. W. Changing patterns of clinical malaria since 1965 among a tea estate population located in the Kenyan highlands. Trans. R. Soc. Trop. Med. Hyg. 94, 253-255 (2000).

39. Rogers, D. J. & Randolph, S. E. Mortality rates and population density of tsetse flies correlated with satellite imagery. Nature 351, 739-741 (1991).

40. Rogers, D. J. A general model for tsetse populations. Insect Sci. Applic. 11, 331-346 (1990).

41. Randolph, S. E. & Rogers, D. J. A generic population model for the Africa tick Rhipicephalus appendiculatus. Parasitology 115, 265-279 (1997).

42. Green, P. E. Analyzing Multivariate Data (The Dryden Press, Hinsdale, IL, 1978).

43. Wolter, K. The Southern Oscillation in surface circulation and climate over the tropical Atlantic, Eastern Pacific, and Indian Ocean as captured by cluster analysis. Clim. Appl. Meteorol. 26, 540-558 (1987).

44. Wolter, K. & Timlin, M. S. Measuring the strength of ENSO-how does 1997/98 rank? Weather 53, 315-324 (1998).

45. Goetz, S., Prince, S. & Small, J. Advances in satellite remote sensing of environmental variables for epidemiological applications. Adv. Parasitol. 47, 289-307 (2000).

46. Rogers, D. J. & Williams, B. G. in Large-Scale Ecology and Conservation Biology (35th Symp. Br. Ecol. Soc./Soc. Conserv. Biol., Univ. Southampton, 1993) (eds Edwards, P. J., May, R. M. & Webb, N. R.) 249-273 (Blackwell Scientific Publications, Oxford, 1994).

47. Rogers, D. J., Hay, S. I. & Packer, M. J. Predicting the distribution of tsetse flies in West Africa using temporal Fourier processed meteorological satellite data. Ann. Trop. Med. Parasitol. 90, 225-241 (1996).

48. Augustin, N. H., Mugglestone, M. A. & Buckland, S. T. An autologistic model for the spatial distribution of wildlife. J. Appl. Ecol. 33, 339-347 (1996).

49. Manel, S., Dias, J. M., Buckton, S. T. & Ormerod, S. J. Alternative methods for predicting species distributions: an illustration with Himalayan river birds. J. Appl. Ecol. 36, 734-747 (1999).

50. Rogers, D. J. & Randolph, S. E. Distribution of tsetse and ticks in Africa: past, present and future. Parasitol. Today 9, 266-271 (1993).